



Early Eocene Arctic volcanism from carbonate-metasomatized mantle

James M. D. Day¹ · D. Graham Pearson² · Bruce A. Kjarsgaard³ · Abigail K. Barker⁴ · Geoff M. Nowell⁵ · Nancy Joyce³ · David Lowry⁶ · Chiranjeeb Sarkar² · Christopher Harrison⁷

Received: 3 July 2023 / Accepted: 15 October 2023
© The Author(s) 2023

Abstract

Melilitite, nephelinite, basanite, and alkali basalt, along with phonolite differentiates, form the Freemans Cove Complex (FCC) in the south-eastern extremity of Bathurst Island (Nunavut, Canada). New $^{40}\text{Ar}/^{39}\text{Ar}$ chronology indicates their emplacement between ~56 and ~54 million years ago within a localized extensional structure. Melilitites and nephelinites, along with phonolite differentiates, likely relate to the beginning and end phases of extension, whereas alkali basalts were emplaced during a main extensional episode at ~55 Ma. The melilitites, nephelinites, and alkali basalts show no strong evidence for significant assimilation of crust, in contrast to some phonolites. Partial melting occurred within both the garnet- and spinel-facies mantle and sampled sources with He, O, Nd, Hf, and Os isotope characteristics indicative of peridotite with two distinct components. The first, expressed in higher degree partial melts, represents a relatively depleted component (“A”; $^3\text{He}/^4\text{He} \sim 8 R_A$, $\varepsilon_{\text{Nd}} \sim +3$, $\varepsilon_{\text{Hf}} \sim +7$, $\gamma_{\text{Os}} \sim 0$). The second was an enriched component (“B” $^3\text{He}/^4\text{He} < 3 R_A$, $\varepsilon_{\text{Nd}} < -1$, $\varepsilon_{\text{Hf}} < +3$, $\gamma_{\text{Os}} > +70$) sampled by the lowest degree partial melts and represents carbonate-metasomatized peridotite. Magmatism in the FCC shows that rifting extended from the Labrador Sea to Bathurst Island and reached a zenith at ~55 Ma, during the Eurekan orogeny. The incompatible trace-element abundances and isotopic signatures of FCC rocks indicate melt generation occurred at the base of relatively thin lithosphere at the margin of a thick craton, with no mantle plume influence. FCC melt compositions are distinct from other continental rift magmatic provinces worldwide, and their metasomatized mantle source was plausibly formed synchronously with emplacement of Cretaceous kimberlites. The FCC illustrates that the range of isotopic compositions preserved in continental rift magmas are likely to be dominated by temporal changes in the extent of partial melting, as well as by the timing and degree of metasomatism recorded in the underlying continental lithosphere.

Keywords Arctic · Eurekan · Rifting · O–Sr–Nd–Hf–Os Isotopes · Ar–Ar geochronology

Introduction

Volcanic and intrusive rocks emplaced within continental rifts span a variety of types from carbonatite to tholeiitic basalt and can vary widely in their isotopic compositions,

an indication of influence from distinct lithospheric and asthenospheric sources (e.g., Le Bas 1987). Relatively common magma series within continental rift volcanics, such as nephelinite, basanite, and basalt are dominantly alkaline and are thought to be generated by partial melting of CO_2 -rich mantle sources (e.g., Brey 1978; Foley 1992). These continental intraplate alkaline volcanic rocks have radiogenic

Communicated by Dante Canil.

✉ James M. D. Day
jmdday@ucsd.edu

¹ Scripps Institution of Oceanography, University of California San Diego, La Jolla, CA 92093-0244, USA

² Department of Earth and Atmospheric Sciences, University of Alberta, Edmonton, AB T6G 2E3, Canada

³ Geological Survey of Canada, 601 Booth Street, Ottawa, ON K1A 0E8, Canada

⁴ Department of Earth Sciences, Uppsala University, 752 36 Uppsala, SE, Sweden

⁵ Department of Earth Sciences, University of Durham, Durham DH1 3LE, UK

⁶ Department of Earth Sciences, Royal Holloway, University of London, Egham TW20 0EX, UK

⁷ Geological Survey of Canada, 3303-33 Street NW, Calgary, AB T2L 2A7, Canada

isotope compositions ranging from those akin to depleted mid-ocean ridge basalt (MORB) to extremely enriched compositions, most especially in the lowest degree potassic partial melts (e.g., Vollmer and Norry 1983; Carlson and Nowell 2001; Carlson et al. 2007). It has been argued that the origin of these exotic compositions is from volatile-rich metasomatized lithosphere (e.g., Foley 1992; Rosenthal et al. 2009; Pfänder et al. 2018), while others have suggested deeper origins for such melts, including within mantle plumes (e.g., Wilson et al. 1995), or from the mantle transition zone (Zeng et al. 2021). Understanding the origin of continental intraplate alkaline volcanic rocks holds importance not only for recognizing passive versus active (i.e., plume influenced) rifting, but for considering regional tectonic processes, and the genesis of diamond-bearing kimberlite volcanism (e.g., Foley et al. 2019).

The Canadian Arctic and Greenland experienced significant volcanic activity during the Cretaceous with emplacement of the High Arctic Large Igneous Province (HALIP; e.g., Tegner et al. 2011; Dockman et al. 2018). This activity was followed—or possibly synchronous with—plate reconfiguration associated with the opening of the North Atlantic and associated basins in the Paleogene that relates to impingement of the Iceland plume beneath Greenland (e.g., Hirschmann et al. 1997; Graham et al. 1998). The FCC volcanic rocks of Bathurst Island in Arctic Canada provide an opportunity to study magma genesis during a period of significant plate tectonic reconfiguration in the Paleogene, where synchronous small-degree melts were intruding the thick central craton (e.g., Sarkar et al. 2015) and its margins.

Eocene volcanic rocks of Bathurst Island (Fig. 1) erupted through continental lithosphere that today displays a strong gradient in thickness, from cool cratonic lithosphere ~ 170 km thick to the south, beneath Somerset Island (e.g., Irvine et al. 2003) to dramatically thinned lithosphere < 80 km beneath the Sverdrup Basin (e.g., Schaeffer and Lebedev 2014; Lebedev et al., 2018). The lithospheric gradient, together with plate tectonic reconstructions suggesting extension followed by compression in the early Eocene, form features of the Eurekan orogeny (Piepjohn et al. 2016; Gion et al. 2017). Despite these lines of evidence, the timing of extension and the potential involvement or influence of HALIP or Iceland plume sources remain unconstrained issues with respect to Eocene Arctic magmatism. Moreover, the timing of events and depths of mantle sources that generated this magmatism offer constraints on the evolutionary history of the lithosphere in the Arctic region between Greenland and northern Canada (Nunavut). We present an integrated petrological, geochronological ($^{40}\text{Ar}/^{39}\text{Ar}$), and geochemical study (including O–Sr–Nd–Hf–Os) of igneous rocks comprising the Freemans Cove Complex (FCC), SE Bathurst Island, to better

understand some of the issues outlined above, including the timing and duration of their emplacement into the crust.

Analytical methods

Mineral chemical analyses were obtained using electron microprobe analyzers at the University of Maryland, College Park and at the Geological Survey of Canada. Bulk rock major element analyses were obtained using X-ray fluorescence at the Geological Survey of Canada, Acme Analytical Laboratories (Canada) and at the University of Leicester (UK), with uncertainty of $< \pm 2\%$ (all reported uncertainties are 2 St. Dev.). Bulk rock trace elements were measured using a *Perkin Elmer* ELAN 6000 inductively coupled plasma mass spectrometer (ICP-MS) at the University of Durham, or for mineral separates at Scripps Institution of Oceanography using an iCAP Qc ICP-MS. Reproducibility is generally better than $\pm 5\%$ for basaltic materials (*Supplementary Information*). Strontium, Nd, and Hf isotope analyses were done at the University of Durham (UK) using a *Thermo* Neptune multi-collector ICP-MS, or for Sr and Nd isotopes at the University of Alberta (UA) using a *Thermo* Triton thermal ionization mass spectrometer. Samples were not leached due to the lack of strong visible alteration for broadly basaltic samples, the risk of removing rare primary carbonate or apatite, or to examine contamination and/or fluid alteration effects on the phonolite samples. Accuracy was determined using both internationally recognized solution and rock standards and precision is better than 30 ppm on $^{87}\text{Sr}/^{86}\text{Sr}$, 35 ppm on $^{143}\text{Nd}/^{144}\text{Nd}$ and 43 ppm on $^{176}\text{Hf}/^{177}\text{Hf}$ (*Supplementary Materials*).

Oxygen isotope analyses were performed on grains of visibly ‘fresh’, inclusion-free olivine, clinopyroxene, and feldspar using a laser fluorination technique. Yield, precision, and accuracy are consistent with previously reported results (e.g., Day et al. 2012; $95 \pm 5\%$ yield, $\pm 0.18\%$ 2SD). Osmium isotope and highly siderophile element (HSE) abundance analyses were performed at Durham University. External precision for $^{187}\text{Os}/^{188}\text{Os}$ was better than 2.1‰ (2SD) with precision and reproducibility of the HSE monitored using basaltic and peridotite reference materials. $^{40}\text{Ar}/^{39}\text{Ar}$ analyses of phenocrysts of sanidine and biotite were performed relative to the Fish Canyon Tuff Sanidine. Irradiation was done at the research reactor of McMaster University and laser $^{40}\text{Ar}/^{39}\text{Ar}$ step-heating analysis was carried out at the Geological Survey of Canada. Detailed methods are provided in the *Supplementary Information*.

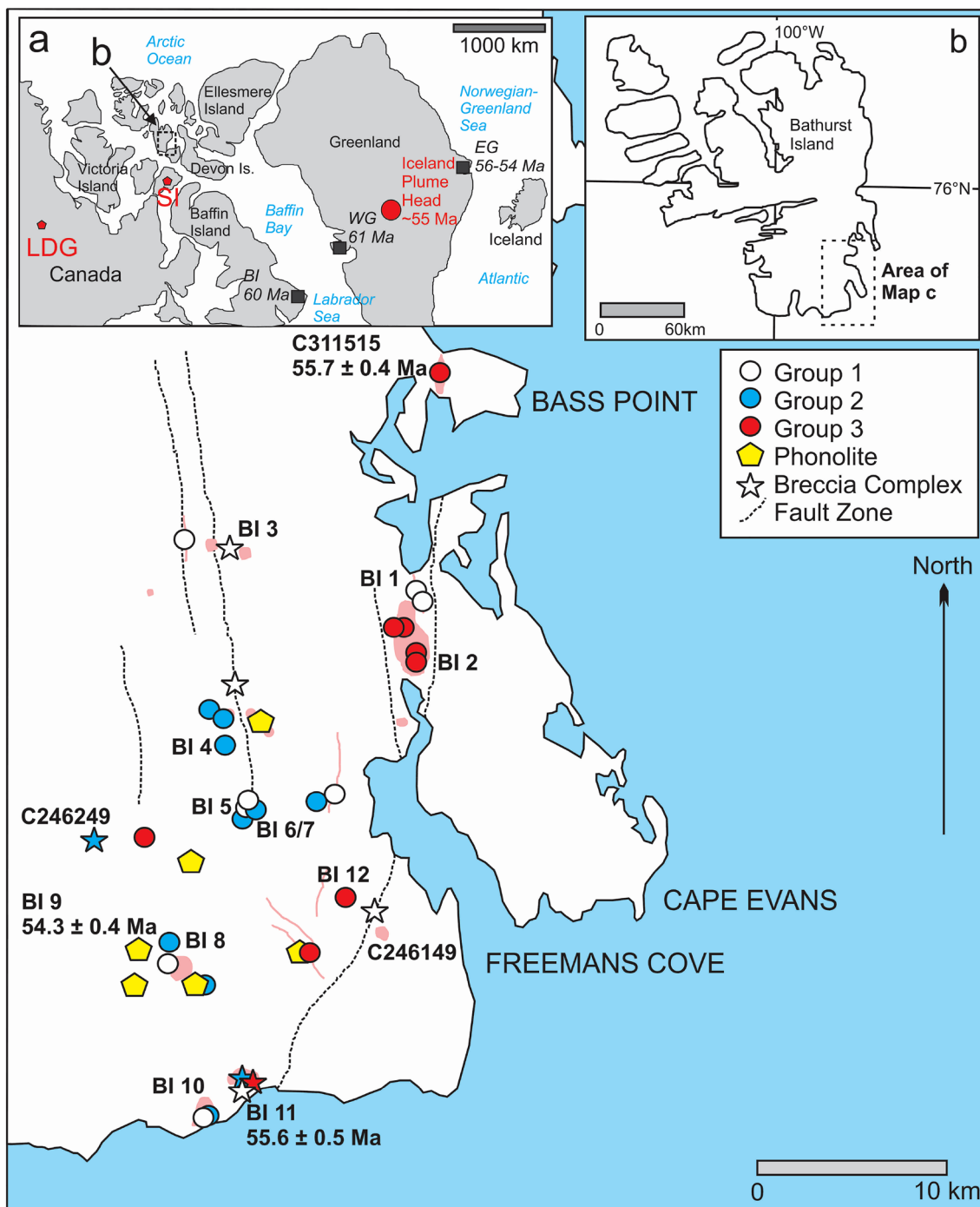


Fig. 1 Map of the Freemans Cove Complex (FCC), Bathurst Island, Canada. Inset (a) shows map of North America with location of Bathurst Island in (b). Main map shows sample locations with samples denoted by grouping (see text for details). Also shown are the Southeast Bathurst Fault Zone and major dike, breccia diatreme and sill complexes. Shown in (a) are locations of kimberlite volcanism

occurring at ~92–100 Ma at Somerset Island (SI), and ~75 to 48 Ma at Lac De Gras (LDG) as well as some features referred to in the text, including the approximate location of the Iceland plume head at ~55 Ma, and East and West Greenland (EG, WG) and Baffin Island (BI) lavas with high-³He/⁴He associated with the Iceland plume

Results

Petrography and mineral chemistry

Detailed sample locations, petrography, and mineral chemistry are presented in *Supplementary Information and Tables*. Field relations and petrology of FCC volcanic rocks have been described previously (Mitchell and Platt 1984), and our observations are consistent with theirs. Volcanic plugs, breccia diatremes, dykes, and sills of the FCC occur along pre-existing reactivated fault structures into a thick succession of Palaeozoic carbonate platform rocks (e.g., Harrison et al. 1998). Samples include nephelinite (including olivine melilite nephelinite), basanite, basalts (grain size > 1 mm, so sometimes referred to as gabbro; Mitchell and Platt 1983, 1984) and phonolites, including ‘mafic’ phonolites that can contain olivine and clinopyroxene (Figure S1). Basalts have generally lower and more variable olivine forsterite contents (Fo_{61-88}) than basanites or nephelinites (Fo_{67-93}) and have lower Ca contents in clinopyroxene (Fig. S2–S3).

Laser fluorination oxygen isotope measurements were performed on olivine, clinopyroxene, and sanidine for melilitite, nephelinite, basanite, alkali basalt, and phonolite from the FCC (Table S4). Mafic samples span a range of olivine $\delta^{18}O$ values (4.5–5.6‰; Fig. 2a). Combined with data for the basanite, the sample set (24 samples measured for olivine, six samples for clinopyroxene) forms a similar distribution of $\delta^{18}O$ to mantle-derived lavas from the Canary Islands (Fig. 2b), with $\delta^{18}O$ for olivine–clinopyroxene pairs being in equilibrium at magmatic temperatures (Fig. 2c). Sanidine from phonolite samples range from ~6.2‰ to values as low as 3.8‰, consistent with hydrothermal alteration of these mineral phases (Weisenberger et al. 2014). The lower $\delta^{18}O$ values of some olivine grains suggest possible assimilation of low- $\delta^{18}O$ contaminants, as observed in Iceland (e.g., Macpherson et al., 2005) and the Azores (e.g., Genske et al. 2013), with the remainder being from melts that are otherwise consistent with mantle-like $\delta^{18}O$. Crush material residual from He isotopic analyses (Day et al. 2005) have olivine REE abundances spanning a similar range of compositions to South African melilitites (Day et al. 2014), but with upturns in the heavy rare earth elements, Ho, Er, Tm, and Yb (HREE; Fig. S4). The FCC span a range in He isotopic compositions (2.4 to 7.1 R_A ; Day et al. 2005) for a relatively restricted range in forsterite numbers.

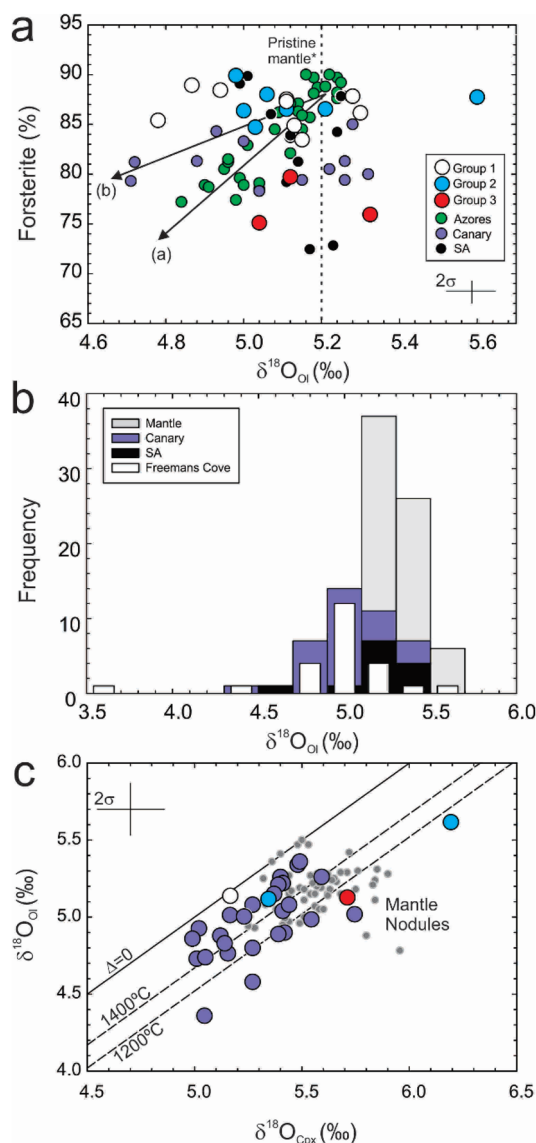


Fig. 2 Plots of **a** olivine $\delta^{18}O$ versus forsterite content; **b** histogram of olivine $\delta^{18}O$ and **c** olivine $\delta^{18}O$ versus clinopyroxene $\delta^{18}O$ for FCC volcanic rocks (Groups 1–3). Vectors in **a** illustrate different postulated low- $\delta^{18}O$ sources involved in some intraplate magmatism, including **(a)** shallow-level assimilation of crust (Genske et al. 2013) and **(b)** sampling of recycled materials with long-term time-integrated variations in radiogenic isotopes (Day et al. 2010). Pristine mantle is the average value taken from the compilation of data by Matthey et al. (1994). Lines in **c** represent isotherms calculated in Zheng (1993). Data sources for **a** and **b** are Azores: Genske et al. (2013), Canary: Day et al. (2010), South Africa (SA): Day et al. (2014). In **b**, **c**, mantle nodule data are from Matthey et al. (1994)

Bulk rock major- and trace-element abundances and groupings

Rocks from the FCC have a range of loss on ignition (0.56–22.6%), reflecting alteration and assimilation of $CaCO_3$ -rich country rock in some instances (e.g., BI3a), or

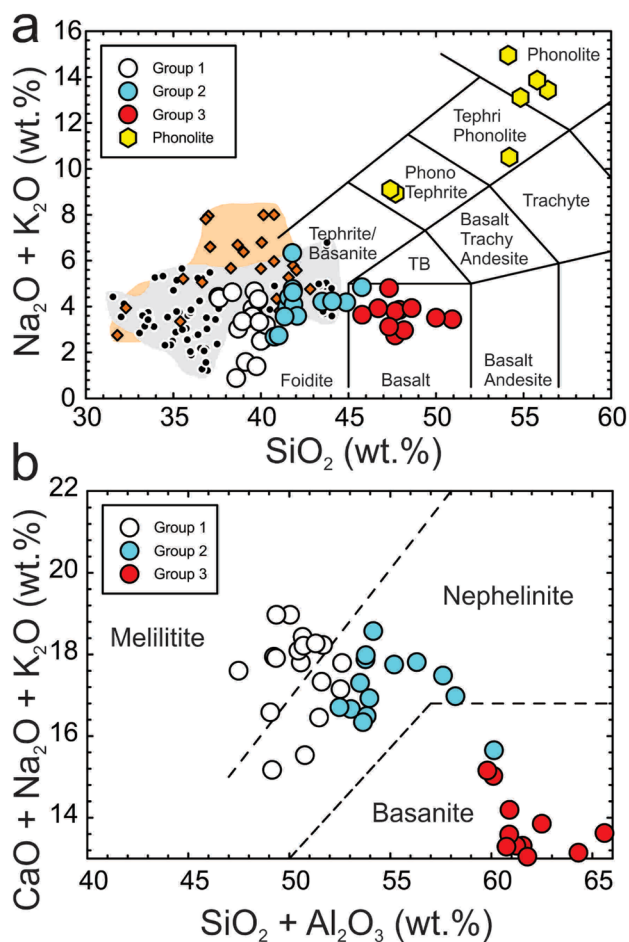


Fig. 3 **a** Total alkalis ($\text{Na}_2\text{O} + \text{K}_2\text{O}$) versus silica diagram for Freeman Cove Complex volcanic rocks (Groups 1–3 and phonolites). Also shown are fields for highly potassic East African Rift lavas (orange diamonds from Rosenthal et al. 2009) and sodic to transitional rocks from the Western Cape Melilitite Province and Namaqualand–Bushmanland–Warmbad lineaments of South Africa (filled dots from Janney et al. 2002, 2003). **b** $\text{CaO} + \text{Na}_2\text{O} + \text{K}_2\text{O}$ versus $\text{SiO}_2 + \text{Al}_2\text{O}_3$ discrimination diagram (Le Bas 1987) showing Group 1 rocks are melilitite to nephelinite, Group 2 are dominantly nephelinites and Group 3 are basanite to alkali basalt

intrinsic volatile contents within nephelinites (Table S6). FCC volcanic rocks range in silica contents (< 30 wt.% to > 57 wt.%), with the melilitite nephelinites being the most silica-poor samples and basalts having 45–51 wt.% SiO_2 . Notably the basalts have a similar range in total alkalis to both the nephelinites and basanites (Fig. 3a), similar to previously reported data (Mitchell and Platt 1984). Mafic samples are subdivided into Group 1 with ≤ 40 wt.% SiO_2 , that range from melilitite to nephelinite, Group 2 that are dominantly nephelinites with 40 to 46 wt.% SiO_2 , and Group 3 that are basanites and alkali basalts (Fig. 3a, b). FCC samples with total alkalis exceeding 8 wt.% range from phono-tephrite, tephri-phonolite, to phonolite in composition and are not grouped as they represent

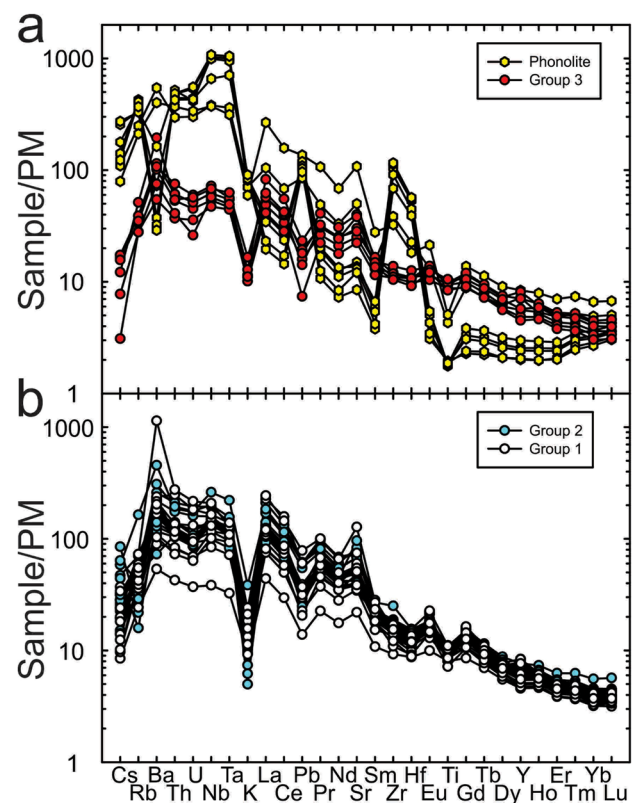


Fig. 4 Primitive mantle (PM) normalized incompatible trace-element diagram for Freeman Cove Complex volcanic rocks broken into **a** phonolites and Group 3 basanites and alkali basalts and **b** Groups 1 and 2 melilitites and nephelinites. Primitive mantle normalization from McDonough and Sun (1995)

compositions after extensive fractional crystallization of more mafic parental melts. FCC nephelinites (up to 18.7 wt.% MgO) and basanites are generally primitive with high Ni contents and low total alkalis and low incompatible (e.g., Zr) element abundances relative to other rocks of similar SiO_2 contents (Fig. S5). Basaltic samples from the FCC span a limited range in MgO (~ 6 to 9 wt.%) and have lower Zr contents than nephelinites and basanites with similar MgO contents, whereas the phonolites have low MgO (< 3 wt.%), Ni (< 30 $\mu\text{g/g}$) and ferric iron and extend to high Zr contents (> 1000 $\mu\text{g/g}$).

Groups 1 and 2 samples (melilitites and nephelinites) have generally elevated large ion lithophile element (LILE) abundances and high Sr (up to 2500 $\mu\text{g/g}$), but otherwise have similar relative primitive mantle (PM)-normalized trace-element compositions to Group 3 basanites and basalts (Fig. 4a, b). Multi-element patterns, with the LILE, rare earth elements (REE), and high field strength elements (HFSE) $> 5 \times \text{PM}$, are typical of continental intraplate alkaline volcanic rocks and all samples have low K/La. Phonolites are characterized by strongly fractionated PM-normalized incompatible trace-element patterns, with high Nb, Ta,

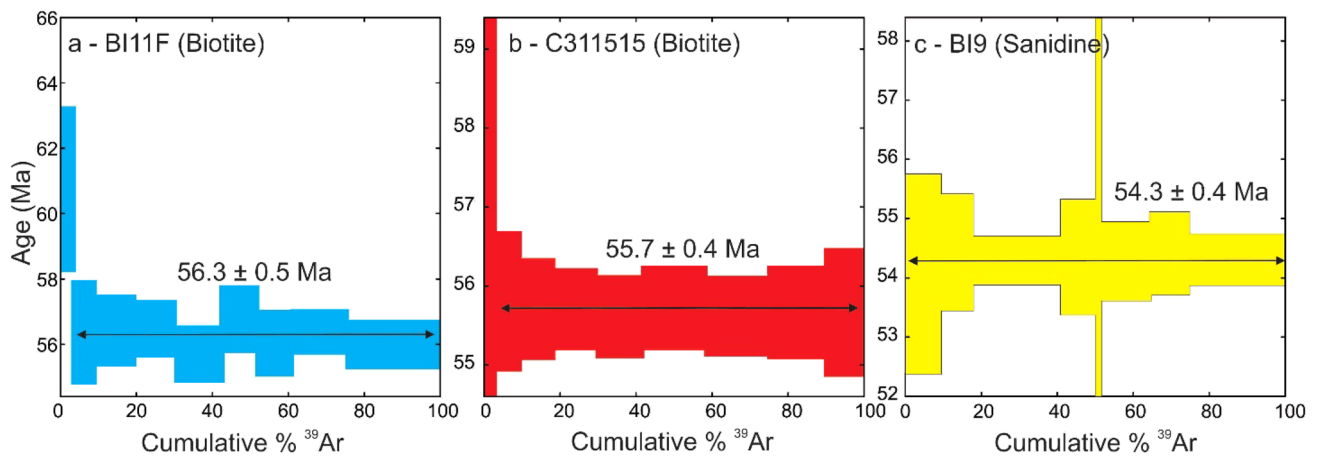


Fig. 5 Argon–argon plateau ages for **a** biotite in Group 2 nephelinite sample BI11F, **b** biotite in Group 3 basanite sample C311515, and **c** sanidine in rhyolite sample BI9. The large low-cumulative % uncer-

tainty measurements in (a) and (b) are not included in the plateau age determinations

Hf, and Zr, but low Ti contents. The incompatible element patterns of the phonolites are typically fractionated but also have flat MREE with flat to elevated HREE and positive Pb anomalies compared to the Group 1–3 samples; these characteristics are consistent with crustal contamination.

Argon-40/Ar-39 chronology

Group 2 nephelinite sample BI11F (biotite), Group 3 basanite sample C311515 (biotite) and phonolite BI9 (sanidine) yield well-defined $^{40}\text{Ar}/^{39}\text{Ar}$ plateau ages, ranging from 56.3 ± 0.5 to 54.3 ± 0.4 Ma (Fig. 5). These age determinations are older and considerably more precise than previous age estimates using ^{40}K – ^{40}Ar and ^{87}Rb – ^{87}Sr (Kerr 1974; Mitchell and Platt 1983), defining the age of the FCC to the very early Eocene. The new Ar–Ar ages are preferred emplacement ages, and all radiogenic data are corrected to an age of 55 Ma.

Strontium–Nd–Hf–Os isotopes

The only previous radiogenic isotope study of FCC samples measured Sr isotopes (Mitchell and Platt 1983). Samples from the FCC have a range in $^{87}\text{Sr}/^{86}\text{Sr}$ (0.70375 to 0.71095), $^{143}\text{Nd}/^{144}\text{Nd}$ (0.51257 to 0.51280), and $^{176}\text{Hf}/^{177}\text{Hf}$ (0.28285 to 0.28293) (Table S7). Age-corrected values range from 0.70362–0.70918 for $^{87}\text{Sr}/^{86}\text{Sr}_i$, -1.9 to $+2.5$ for ϵNd_i and $+3.6$ to $+6.7$ for ϵHf_i , with $\Delta\epsilon\text{Hf}_i$ ($\epsilon\text{Hf}_i - ((\epsilon\text{Nd}_i \times 1.33) + 3.19)$) from -5.6 to -0.5 . In contrast to previous studies (Mitchell and Platt 1983), no isochronous relationships exist for $^{87}\text{Rb}/^{86}\text{Sr}$ – $^{87}\text{Sr}/^{86}\text{Sr}$, or for $^{147}\text{Sm}/^{144}\text{Nd}$ – $^{143}\text{Nd}/^{144}\text{Nd}$, or $^{176}\text{Lu}/^{177}\text{Hf}$ – $^{176}\text{Hf}/^{177}\text{Hf}$. In Sr–Nd isotope space, most FCC samples have a large range of ϵNd_i for a limited range in $^{87}\text{Sr}/^{86}\text{Sr}_i$ (Fig. 6a, b). Exceptions are some

phonolites (C311463, C311465, C311472) that have variably radiogenic $^{87}\text{Sr}/^{86}\text{Sr}_i$ up to 0.709. All FCC samples lie above the terrestrial mantle array in Nd–Hf isotope space indicating higher long-term time-integrated Lu/Hf than Sm/Nd, similar to some Lac de Gras kimberlites (Fig. 6c, d).

Ten FCC samples are reported for Re, Os, and ^{187}Re – ^{187}Os , with a subset of samples also characterized for Ru \pm Pd \pm Pt and Ir (Table S8). Concentrations of Os and Re in FCC samples vary from 0.011 to 0.207 ng/g and 0.119 to 1.47 ng/g, respectively, with measured $^{187}\text{Os}/^{188}\text{Os}$ from 0.145 to 0.273, corresponding to γOs_i of -1 to $+63$ (Fig. 7). FCC samples are not isochronous. Instead, a Group 3 sample (BI 12) defines a 55 Ma model age, whereas Groups 1 and 2 samples have radiogenic initial Os (Fig. S6a). Primitive mantle-normalized HSE patterns are generally fractionated for Ru, Ir, and Os, relative to Pd, Pd, and Re, consistent with previous measurements of continental intraplate alkaline volcanic rocks (Day 2013) (Fig. S6b). Samples from the FCC generally have low Os contents and a range in γOs_i similar to South African melilitites (Janney et al. 2002; Fig. 7), but do not extend to the high γOs_i of Colorado Plateau potassic magmas, or the high Os contents of some East African Rift potassic lavas.

Discussion

Age of the FCC, duration of magmatism, and regional context

Previous efforts to date the FCC have used ^{40}K – ^{40}Ar determinations on ‘keratophyre’ (60 ± 3 Ma and 47 ± 8 Ma; Kerr 1974), or used bulk-rock ^{87}Rb – ^{87}Sr systematics for nephelinites and phonolites (47.1 ± 4 Ma; calculated to

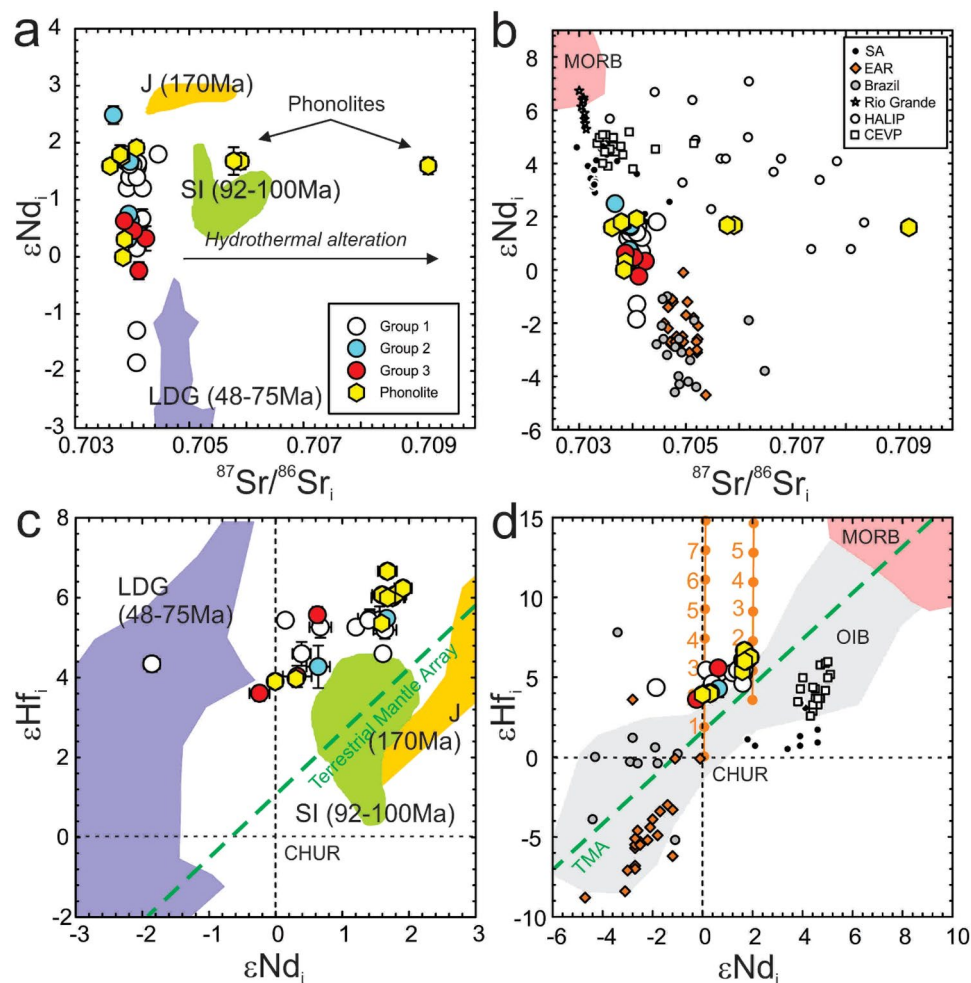


Fig. 6 Initial **a**, **b** $^{87}\text{Sr}/^{86}\text{Sr}_i$ versus ϵNd_i and **c**, **d** ϵNd_i versus ϵHf_i for FCC volcanic rocks compared to kimberlites from the Lac de Gras (LDG), Jericho (J), and Somerset Island (SI) pipes (data from Dowall 2004; Tappe et al. 2013; Kjarsgaard et al. 2017), major volcanic rock types (mid-ocean ridge basalt [MORB] and ocean island basalt [OIB]), as well as South African (SA) melilitites (Janney et al. 2002; Janney and Roex 2003), East African Rift (EAR) volcanic rocks (Rosenthal et al. 2009), Brazilian kamafugites (Carlson et al. 2007), Rio Grande rift basanites (Thompson et al. 2005), Central European Volcanic Province basanites (CEVP; Pfänder et al. 2018), and High

Arctic LIP (Dockman et al. 2018). FCC volcanic rocks are broken into Groups 1–3 samples and phonolite differentiates. Shown in **c**, **d** are the Chondritic Uniform Reservoir (CHUR) compositions for Nd–Hf isotopes (Bouvier et al. 2008) and the Terrestrial Mantle Array, defined as $\epsilon\text{Hf}_i = 1.44 \times \epsilon\text{Nd}_i + 1.61$ (Vervoort et al. 1999). In **d** are ingrowth models (orange lines with dots) for a carbonate-metasomatized source with extreme Lu/Hf (20) and Sm/Nd of between 0.05 and 0.2 from Bizimis et al. (2003) assuming a CHUR-like starting composition and a more depleted source. Numbers for this model are in millions of years

47.9 Ma using updated ^{87}Rb decay constant; Mitchell and Platt 1983). These ages indicate the emplacement of the FCC during the Paleocene and the middle Eocene. The new data from this study suggest that the ^{87}Rb – ^{87}Sr bulk-rock isochron from Mitchell and Platt (1983) does not provide a reliable age estimate for the FCC (e.g., Fig. S7). Samples span a range of $^{87}\text{Sr}/^{86}\text{Sr}$ for a limited range in $^{87}\text{Rb}/^{86}\text{Sr}$, with the most extreme variations recorded in phonolites (Fig. 6). Some phonolites fall within the range of a 55 Ma isochron line anchored to the lowest measured $^{87}\text{Sr}/^{86}\text{Sr}$. Others, however, have highly radiogenic $^{87}\text{Sr}/^{86}\text{Sr}$ for a given $^{87}\text{Rb}/^{86}\text{Sr}$ ratio, lying above the isochron. This indicates that

bulk-rock Rb–Sr isochron determinations are unlikely to be reliable from crustally modified phonolites that also have variable O isotope compositions and elevated Tm, Yb, Lu, and Pb.

The $^{40}\text{Ar}/^{39}\text{Ar}$ ages from the three FCC samples span a restricted age range (56.3 ± 0.5 Ma to 54.3 ± 0.4 Ma), indicating an early Eocene age (Fig. 5; Table S9). Using the maximum and minimum age uncertainties, the distribution in these ages suggests a possible eruption duration of 2.9 to 2.2 Myr, respectively. Notably a basanite sample (C311515, 55.7 ± 0.4 Ma) has an age intermediate to nephelinite and phonolite, permissive with more Si-saturated samples

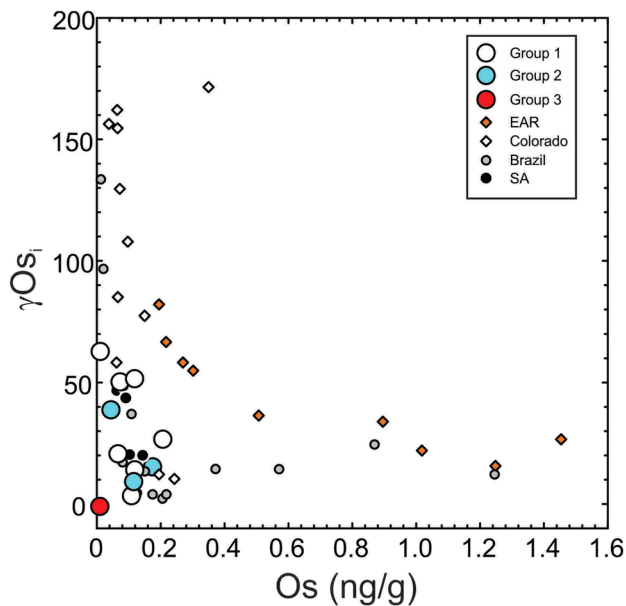


Fig. 7 Osmium concentration versus age-corrected γOs for Freemans Cove Complex samples (Groups 1–3) versus other data from the East African Rift (EAR; Rosenthal et al. 2009), Colorado (Carlson and Nowell 2001), Brazil (Carlson et al. 2007), and South Africa (SA) (Janney et al. 2002)

erupting at intermediate periods to more Si-undersaturated rocks. We contend that the reported $^{40}\text{Ar}/^{39}\text{Ar}$ ages are the crystallization age for FCC rocks, with the duration of magmatism slightly exceeding 2 Myr, from ~56 to ~54 Ma. The early Eocene age of the FCC places it as being distinct from the tholeiitic stage of the HALIP, associated with extension at 130 to 80 Ma (e.g., Dockman et al. 2018). The FCC is also too young to be associated with the alkaline suite attributed to continental rifting in the Lincoln Sea area at 85–60 Ma (e.g., Tegner et al. 2011). This latter feature of the HALIP has been suggested to be distinct from the earlier tholeiitic stage, and possibly more consistent with Eurekan deformation (Tegner et al. 2011). The 54–56 Myr age places FCC magma emplacement contemporaneous with the main phase of Eocene diamondiferous kimberlite eruptions on the cratonic foreland of the Slave craton (Sarkar et al. 2015). The age of the FCC also overlaps with the age of basaltic magmatism in both western and eastern Greenland (~53 to 55 Ma; e.g., Tegner et al. 1998; Hirschmann et al. 1997).

A parsimonious cause for initiation of FCC magmatism is through Eurekan deformation associated with Arctic plate reconfigurations due to inception of seafloor spreading both west and east of Greenland (Gion et al. 2017; Piepjohn et al. 2016). Intra-continental deformation associated with the Eurekan orogeny began at ~63 Ma with extension between Ellesmere and Devon Island (Fig. 1) that lasted until ~55 Ma, followed by north–south compression at Ellesmere Island (Gion et al. 2017). Eurekan deformation

is known to have resulted in reactivation of Palaeozoic structures as strike-slip fault zones in the Circum-Arctic region (Piepjohn et al. 2016). In addition, it has been proposed that faulting in eastern Bathurst Island might relate to Eurekan deformation in the eastern Arctic Islands (e.g., Harrison 2018). Emplacement of FCC volcanic rocks at ~56 to 54 Ma supports reactivation of pre-existing fault structures during a period of extension at SE Bathurst Island. As such, FCC emplacement offers insights into tectono-magmatic processes occurring in the Arctic during the Eocene, demonstrating that an extensional component of deformation occurred in the region. The FCC formed with an absence of high- $^3\text{He}/^4\text{He}$ (Day et al. 2005), in contrast to the high- $^3\text{He}/^4\text{He}$ measured in Baffin Island, West and East Greenland lavas erupted at around this time (e.g., Marty et al., 1998; Graham et al. 1998; Stuart et al. 2003). This striking difference between the Baffin/West Greenland Eocene magmas and FCC magmatism indicates that in the region of Bathurst Island, crustal extension was in response to plate tectonic reconfiguration, rather than being driven by impingement of a mantle plume.

Alteration and assimilation of crust

The FCC was emplaced into a series of folded and deformed sedimentary rocks of Ordovician to Devonian age that are up to 8 km thick (Kerr 1974; Harrison 2018). Evidence for crustal assimilation is observed in the field where breccia agglomerates (e.g., BI 3a) preserve mechanical mixing of limestone blocks, demonstrating shallow-surface assimilation took place in certain instances. In addition, phonolites are strongly altered (also noted by Mitchell and Platt 1984), consistent with fluid alteration and crustal modification, specifically for Sr, Pb, MREE, and the HREE. Petrographic observations of nephelinites and basanites with vugs filled by zeolite (e.g., BI5, C246247) or calcite (C246156), iddingsite and/or serpentine within olivine (e.g., BI8, BI10C, BI10G) all indicate some degree of alteration in samples. Glomerocrystic rafts of olivine and/or clinopyroxene within samples are consistent with magma fractionation and accumulation processes (*Supplementary Information*), whereas strained olivine grains (e.g., BI5, BI8) may represent xenocrysts.

Phonolites are most strongly affected by post-crystallization alteration. Some samples (C311463, C311465, C311472) have radiogenic $^{87}\text{Sr}/^{86}\text{Sr}$ yet similar Rb/Sr to other phonolites with lower $^{87}\text{Sr}/^{86}\text{Sr}$, with no corresponding variation in ϵ_{Nd} (Fig. 6). The systematics are consistent with hydrothermal alteration and addition of radiogenic Sr from limestone. Ordovician to Devonian marine carbonates can have high Sr contents, with $^{87}\text{Sr}/^{86}\text{Sr}$ as high as 0.7095 (Veizer 1989), consistent with the Sr isotopic compositions of the most radiogenic

phonolites. Oxygen isotopes are sensitive to crustal assimilation processes, and in high latitude regions, the low $^{18}\text{O}/^{16}\text{O}$ of meteoric water can lead to incorporation of low- $\delta^{18}\text{O}$ in melts during assimilation of hydrated altered crust (e.g., Taylor and Forester 1971). For the FCC basaltic rocks, olivine compositions mostly fall around a mantle-like $\delta^{18}\text{O}$ composition, and olivine–clinopyroxene pairs are generally in equilibrium at high temperatures. There is, however, a prominent tail to low- $\delta^{18}\text{O}$, specifically in phonolite C311455, and nephelinites B111C and B110E, with some samples falling along trends permissive of shallow-level assimilation of crust. Sanidine crystals yield low- $\delta^{18}\text{O}$ in phonolites (e.g., C311458, C311463, B19) supporting the assimilation of hydrated crustal materials, or extensive interaction with crustal fluids. Alteration and crustal contamination effects are not ubiquitous to all FCC rocks; however, most Group 1–3 samples have mantle-like $\delta^{18}\text{O}$ and limited evidence for either process acting upon them. For example, these rocks have consistently negative Pb anomalies, relative to Ce and Pr (Fig. 4) and $\text{Ce}/\text{Pb} > 20$ and $\text{Nb}/\text{U} > 38$, consistent with limited crustal or fluid-dominated alteration (e.g., Pfänder et al. 2018). For the Group 1, 2 and 3 samples, lack of obvious evidence for crustal contamination for Sr–Nd–Hf–Os isotopes and correlations between trace elements that exist for indicators of magmatic differentiation (MgO), but not for alteration (e.g., LOI) all indicate limited crustal assimilation or alteration affecting these rock types.

Fractional crystallization processes are responsible for the evolved FCC rock types. These effects are evident in bulk-rock compositions and in olivine compositions, with decreasing Ni and increasing Mn and Ca with decreasing forsterite content in all rock types (e.g., Figs. S2, S3, S8). Furthermore, a range of olivine compositions for Group 1–3 samples provide evidence for the presence of phenocrysts, fractionated groundmass, and xenocrysts in samples (Supplementary Information) suggesting that, while fractional crystallization is significant in some samples, many represent either primitive melts or melts that incorporated antecrysts and/or potentially rare xenocrysts. An example of significant fractional crystallization is the formation of the phono-tephrite, tephri-phonolites, and phonolites that can be explained by crystallization of parental melts similar to nephelinite or basanite. It is more difficult to explain the relationship of the Group 3 samples to Groups 1 and 2 samples through fractional crystallization; Group 3 samples have a similar total alkali content for a given silica content (Fig. 3) and are also characterized by low Zr for a given MgO content, as well as lower LREE/HREE ratios. These magma types require variability in primitive melt compositions, as discussed below.

The roles of processes including post-crystallization alteration, crustal assimilation, and fractional crystallization

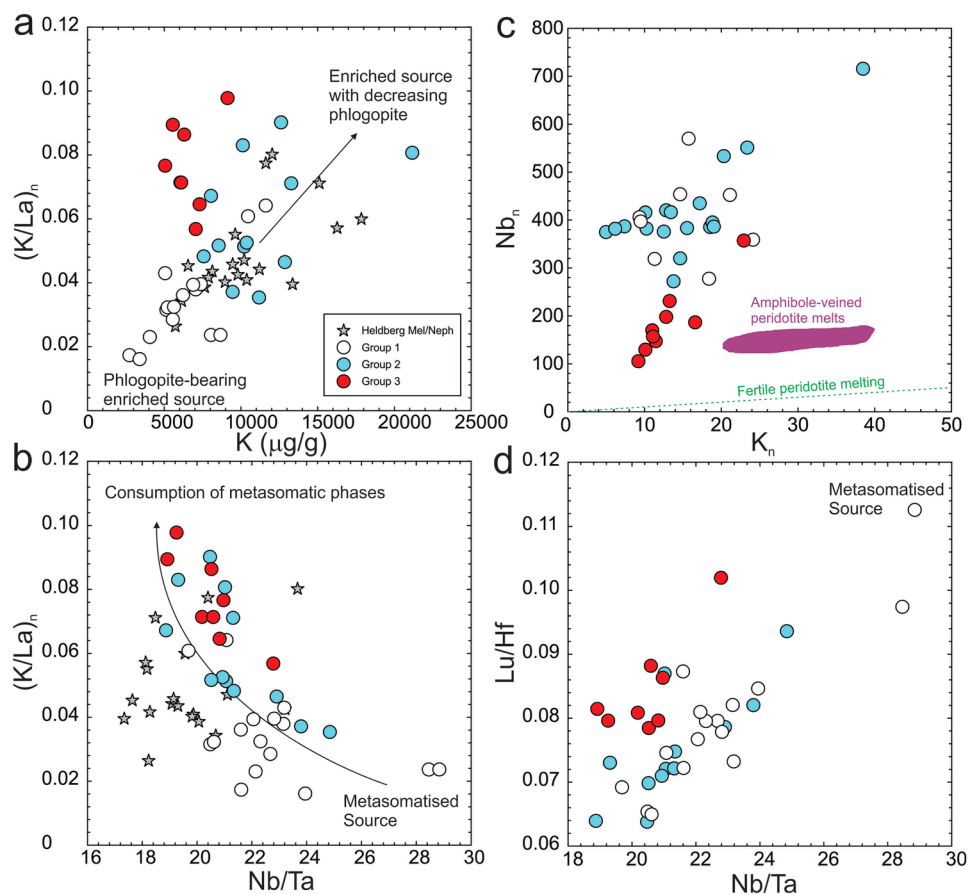
on FCC volcanic rock compositions are in some cases extreme, such as for phonolites and breccia agglomerates, but there is no strong petrological, trace element or isotopic evidence to demonstrate that these processes discernibly affected Groups 1, 2 or 3 samples that we focus on for determining source compositions. Instead, Group 1–3 samples broadly reflect the composition of the mantle-derived melts that produced them, as noted by Mitchell and Platt (1983; 1984).

Phlogopite and amphibole in a carbonate-bearing mantle source

Volcanic rocks from the FCC have previously been shown to share broad similarities in the style of magmatism with other continental intraplate alkaline volcanic rocks (Mitchell and Platt 1984), including the Balcones Province, Texas (Spencer 1969), the Rhine Graben (e.g., Brey 1978; Wilson et al. 1995; Blusztajn and Hegner 2002; Jung et al. 2011; Pfänder et al. 2018), and magmatism in eastern Australia (Frey et al. 1978). The FCC also has similarities to continental intraplate alkaline volcanic rocks from South Africa (e.g., Janney et al. 2002, 2003), as well as to the melts that intruded the Colorado Plateau (Carlson and Nowell 2001), Brazil (Carlson et al. 2007), and the East African Rift (Rosenthal et al. 2009). The sources of anomalous isotopic compositions in these locations have been attributed to processes including crustal contamination (e.g., Jung et al. 2011), or contributions of melts from mantle plumes, or the mantle transition zone (e.g., Wilson et al. 1995; Zeng et al. 2021). The most common sources for continental intraplate alkaline volcanic rocks generally involve non-cratonic continental lithosphere (e.g., Blusztajn and Hegner 2002), containing variably enriched isotopic components, such as mafic lithospheric rocks (c.f., pyroxenite; Carlson and Nowell 2001), or metasomes with distinct signatures (carbonatite-, phlogopite-, or amphibole-enriched volatile-rich metasomatized lithosphere, e.g., Foley 1992; Rosenthal et al. 2009; Pfänder et al. 2018). The volatile-rich nature of some of these latter proposed sources are consistent with the requirement for CO_2 -rich mantle sources to form melilitite and nephelinite (e.g., Brey 1978), that would also facilitate partial melting.

A likely average depth of partial melting for the FCC is ~ 100 km, based on surrounding lithospheric thickness estimates and with phase equilibria studies (e.g., Brey 1978). Group 1 samples have the lowest K and low $(\text{K}/\text{La})_n$ that also correspond to some of the highest Nb/Ta compositions (Fig. 8a, b). Groups 1 and 2 samples also have more elevated Nb/K than Group 3 samples and all have higher than expected Nb/K than for melts generated from fertile peridotite melting (e.g., Ball et al. 2019; Canil et al. 2021; Fig. 8c). The signature of low K/La and high Nb/Ta, Nb/K,

Fig. 8 Examining phlogopite, amphibole, and carbonate in mantle sources. **a** Potassium content versus PM-normalized K/La, **b** Nb/Ta versus PM-normalized K/La, **c** Primitive mantle-normalized K and Nb abundances, and **d** Lu/Hf versus Nb/Ta. Shown in **c** is fertile peridotite melting model of Ball et al. (2019) and field for amphibole-veined peridotite melts from Pilet et al. (2008). Data for Heldberg melilitites and nephelinites (Rhine Graben) and interpretations are from Pfänder et al. (2018). Only broadly basaltic Group 1–3 FCC volcanic rocks are shown on these plots due to the extreme differentiation experienced by FCC phonolites



and Lu/Hf suggests sourcing of Group 1 rocks from metasomatized peridotite containing residual phlogopite and, possibly, amphibole (Fig. 8d). With increasing extents of partial melting, these metasomatized components were either diluted or exhausted in a manner akin to Rhine Graben continental intraplate alkaline volcanic rocks (Pfänder et al. 2018). Another striking characteristic of FCC magmatic rocks is that, unlike other continental intraplate alkaline volcanic rocks, all lie above and to the left of the Hf–Nd isotope mantle array (Fig. 6). It has previously been shown that magmatic carbonates have high Lu/Hf (Bizimis et al. 2003) and so will generate radiogenic Hf isotope compositions relative to Nd, like those required to generate FCC partial melts. Using the pure carbonate composition of Bizimis et al. (2003; Lu/Hf = 20, Sm/Nd = ~0.05–0.2) would lead to ingrowth to FCC-like compositions from an initially chondritic composition within 2–3 Myr (Fig. 6d). Assuming ~5% carbonate in the mantle would extend ingrowth proportionally to ~40 Ma, indicating that such a source would be relatively short lived.

A notable feature of Group 3 samples is that they have higher SiO₂ for a given total alkali content than Group 1 or 2 nephelinites (Fig. 3), reflecting different degrees of silica saturation. Mitchell and Platt (1984) noted a similar

relationship and proposed five different magma series in the FCC, that can be broadly expressed as silica-undersaturated magmas (nephelinites, basanites, phonolites) and more silica-rich magmas (basalts or gabbro). The differences in these magma types are evident in trace-element abundances, where Group 3 samples have flatter REE patterns ($[La/Yb]_n = 20 \pm 12$) than Groups 1 or 2, with $(La/Yb)_n = 32 \pm 10$ (Fig. 4). Differences between Groups 1 and 2 versus Group 3 samples could reflect degree of partial melting, partial melting initiation depth (which is mostly influenced by lithosphere thickness in the absence of anomalous mantle potential temperatures, e.g., McKenzie and Bickle 1988), distinct mantle sources, or a combination of these factors. A wide variety of FCC volcanic rock compositions were erupted within a restricted geographic region (~40 × 20 km²), however, suggesting that variability in lithospheric thickness did not play a major role in the extent of partial melting. This is, of course, unless there was a rapid temporal variation in lithospheric thinning, although evidence of this process is absent. Furthermore, the melts responsible for the erupted volcanic rocks do not appear to have been anomalously hot (Group 1 = 1220 ± 60 °C; Group 2 = 1240 ± 60 °C; Group 3 = 1150 ± 25 °C; using the simplified method of Nisbet et al. 1993).

Alternatively, temporal variation in the magnitude of extension and concomitant exhaustion of carbonate–phlogopite \pm amphibole in the mantle source may have been more important in the degree of partial melting. Evidence for this includes the likelihood of prolonged magmatism in the FCC, of around 2 Myr, as well as the intermediate age of Group 3 (basanite sample C311515) relative to the older silica-undersaturated Group 2 nephelinite (BI11F) and younger phonolite (BI9), permissive of the main phase of extension occurring at ~ 55.7 Ma, with more limited extension before > 56 Ma and after this period $< \sim 54.3$ Ma. This suggests that extent of partial melting may have been most important in the distinction between Groups 1 and 2 versus Group 3 samples. For illustration, partial melt models were constructed for the REE (Supplementary Information) assuming relatively enriched mantle sources. The exact parameters of source modal mineral abundances and phase melting proportions, mineral partition coefficients, calculated bulk and liquid partitioning and concentration of elements in the source are listed in *Table S10*. The first enriched mantle source composition was assumed to be like primitive mantle (i.e., chondritic La/Yb and Dy/Yb ratios) and the second was a LREE-enriched source, consistent with phlogopite-rich metasomatized mantle (Fig. 9). The models assume phlogopite in the source at depth, but none in the shallower (spinel-facies) mantle. For the purpose of the models, amphibole has been excluded and, as such the models provide only an illustration of the likely degrees of partial melting and mantle source composition. Based on these calculations, the enriched phlogopite-bearing source (En. S) will generate higher degree partial melts relative to

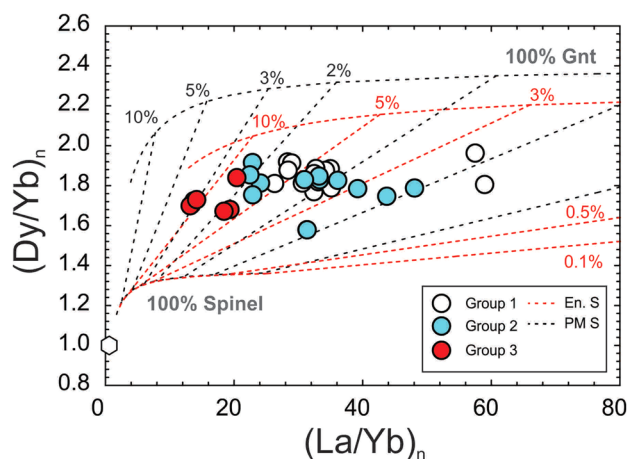


Fig. 9 Estimates of partial melting for high-MgO (> 8 wt.%) FCC samples (Group 1–3) versus the typical N-MORB composition (unfilled hexagon). The model assumes a primitive mantle source (PM S) and an enriched mantle source containing phlogopite (En. S). Modeling details are provided in *Table S10*. Percentage values of the different models reflect the degrees of partial melting at 100% spinel facies melting and 100% garnet facies melting

a PM-like source (Group 1 and 2: PM S = 0.5– $> 2\%$; En. S = 2– $> 5\%$; Group 3: PM S = 2–3%; En. S = 5–10%). In all cases, Group 3 magmas require higher degrees of partial melting. The similarity of elevated Hf for a given Nd isotope composition for all FCC magmas indicates that mantle sources tapped by the magmas were broadly the same, but that Group 3 magmas had contributions from a distinct source component not evident in Groups 1 and 2 samples. These results suggest a depleted mantle source with components that were fusible within it, perhaps most similar to a veined and heterogeneously metasomatized mantle.

Timing of metasomatism, mantle source expressions, and comparison with global continental intraplate alkaline volcanic rocks

Samples from the FCC have Sr–Nd–Hf–Os isotope compositions distinct from other global examples of continental intraplate alkaline volcanic rocks. They lie intermediate to South African and Central European Volcanic Province (CEVP) melilite-bearing rocks and East African Rift (EAR) or Brazilian potassic rocks in Sr–Nd–Hf isotope space (Fig. 6) and have generally less radiogenic Os for a given Os content than potassic equivalents (Fig. 7). The majority of silica-undersaturated continental intraplate alkaline volcanic rocks are thought to originate from the thermal boundary layer (TBL)—the region of the lithosphere between the convecting asthenosphere ($> 1250^\circ\text{C}$) and the mechanical boundary layer (MBL) of the lithosphere—where mantle rocks behave rigidly ($< 750^\circ\text{C}$; e.g., Wilson et al. 1995; Thompson et al. 2005). As such, the TBL is not at a fixed depth/pressure but is of variable depth due to the degree of lithospheric thinning. The FCC sampled a broadly enriched mantle source based on Sr–Nd–Hf–Os isotopes, distinct from earlier (130–80 Ma) mantle sources of HALIP (Fig. 6; e.g., Dockman et al. 2018), and more enriched than partial melts from the Rio Grande (e.g., Thompson et al. 2005). The FCC mantle source region is less enriched than low-degree partial melts from the EAR, Brazil, the Rhine Graben, or the Colorado Plateau (e.g., Carlson and Nowell 2001; Carlson et al. 2007; Rosenthal et al. 2009; Pfänder et al. 2018). Greatest similarities exist between FCC Hf isotopic compositions and the extreme compositions of a subset of Lac De Gras kimberlites (Fig. 6).

Trace-element geochemistry, mantle-like $\delta^{18}\text{O}$, low $^{87}\text{Sr}/^{86}\text{Sr}_i$ (~ 0.704), high $\epsilon_{\text{Hf}i}$ for a given $\epsilon_{\text{Nd}i}$ (Fig. 6) and variable but high $\gamma_{\text{Os}i}$ of FCC volcanic rocks are consistent with melting of both relatively depleted and enriched mantle reservoirs. Negative covariations between PM-normalized La/Yb—a proxy for partial melting processes—and $\epsilon_{\text{Hf}i}$ and $\epsilon_{\text{Nd}i}$, and a positive correlation with $\gamma_{\text{Os}i}$ illustrate that Groups 1 and 2 parental melts preferentially sampled the more enriched metasomatized mantle reservoir (Fig. 10a,b;

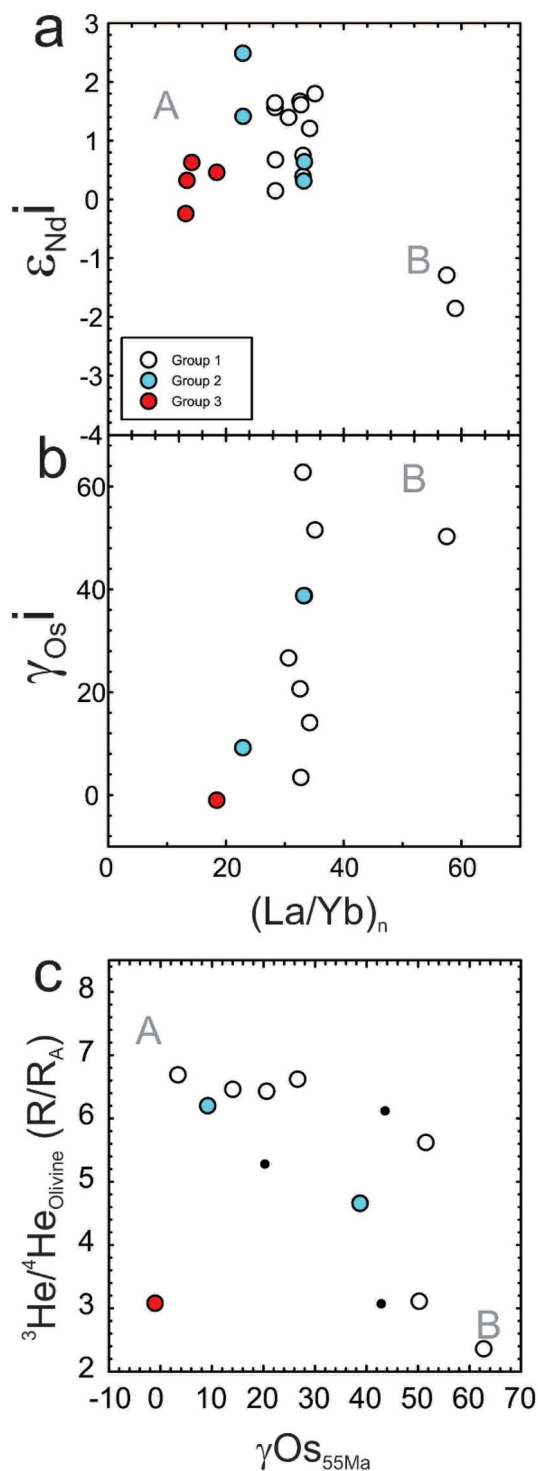


Fig. 10 Illustration of source components (A) and (B) within the FCC mantle. Primitive mantle-normalized La/Yb versus age-corrected ϵ_{Nd} and **b** γ_{Os} for FCC volcanic rocks (Groups 1–3). **c** Shows age-corrected γ_{Os} versus ${}^3\text{He}/{}^4\text{He}$ determined from crushing olivine for FCC volcanic rocks. Helium isotope data for these rocks are from Day et al. (2005) and include South African melilitites (small, filled circles)

Fig. S9). Notably, $\epsilon_{\text{Nd}i}$ and $\gamma_{\text{Os}i}$ negatively covary (Fig. S10) in the FCC, which is not observed in other low-degree partial melts, such as those from the EAR or Brazil. There is also a negative covariation with $\gamma_{\text{Os}i}$ and ${}^3\text{He}/{}^4\text{He}$ (Fig. 10c). Previously, Day et al. (2005) showed that many continental intraplate alkaline volcanic rocks have low ${}^3\text{He}/{}^4\text{He}$. The relationship of low-degree partial melts having low ${}^3\text{He}/{}^4\text{He}$ ($< 3 R_A$) further suggests that the TBL is the source of low ${}^3\text{He}/{}^4\text{He}$. These arguments and Nd–Hf isotope modeling (Fig. 6d) indicate that Bathurst Island mantle lithosphere was likely metasomatized sometime between the Cretaceous and Eocene by volatile-rich melts or fluids that formed carbonated phlogopite + amphibole peridotite that was later partially melted during extension to form FCC magmatism.

The covariation of Nb/Ta and Lu/Hf in FCC samples (Fig. 8d) is consistent with a peridotite source containing phlogopite + carbonate + amphibole. We propose that carbonation of this source, from metasomatism, could have happened shortly prior to FCC magmatism, or ~ 40 Ma earlier, during a phase of regional magmatism that led to the formation of the nearby Cretaceous kimberlites at Somerset Island (~ 95 Ma; Kjarsgaard et al. 2017). Somerset Island mantle peridotite xenoliths (~ 250 km to the southeast of Bathurst Island) have petrographic and geochemical characteristics consistent with late-stage oxidizing carbonate metasomatism at ~ 90 Ma (Gräf et al. 2019). If similar metasomatism stabilized carbonate beneath the Bathurst Island lithosphere, it could account for the divergence of FCC volcanic rocks from the Hf–Nd isotope mantle array. A driver for this Cretaceous metasomatism could be the wide-spread effects, beneath thicker lithosphere, of the HALIP magmatic event (Dockman et al. 2018) that metasomatically primed the mantle beneath Bathurst Island, rather than producing magmatism at the surface. It is, therefore, plausible that the source of FCC magmas was metasomatized by melts associated with the Somerset Island kimberlites and then aged for 35–40 Ma, prior to formation of the FCC. Melting could have been triggered by a small-scale convective instability related to a severe gradient in lithospheric thickness in this region of the Canadian Arctic (e.g., Lebedev et al. 2018).

Based on the relationships of Groups 1, 2, and 3 samples, it is possible to determine likely endmember compositions for the sampled mantle components. The first reservoir (A) is expressed in low La/Yb_n samples, which are characterized by MORB-like ${}^3\text{He}/{}^4\text{He}$ ($\sim 8 R_A$), broadly chondritic ${}^{187}\text{Os}/{}^{188}\text{Os}$, $\epsilon_{\text{Nd}i}$ of $\sim +3$, and $\epsilon_{\text{Hf}i}$ of $\sim +7$ (Fig. 10). These higher degree melts formed the Group 3 basalts and basanites. Apart from the relatively unradiogenic Nd isotope composition of this endmember, it appears similar to depleted MORB mantle (DM). A particularly notable aspect of this endmember is the absence of definitive evidence for a sub-chondritic Os isotope signature that characterizes

cratonic mantle peridotite xenoliths to the southeast and southwest of the FCC (Irvine et al. 2003; Liu et al. 2018) suggesting it is not Archaean cratonic lithosphere. In contrast, the most unradiogenic Os isotope compositions for the FCC are close to chondritic and the endmember may be a mixture of DM from asthenospheric contributions and unmetasomatized non-cratonic lithosphere. The second reservoir (B) is identified in the lowest degree partial melts (e.g., Groups 1 and 2 melilitite and nephelinite) and has low $^3\text{He}/^4\text{He}$ ($< 3 R_A$), elevated $^{187}\text{Os}/^{188}\text{Os}$ ($\gamma_{\text{Os}i} = > +70$), and unradiogenic Nd–Hf isotope systematics ($\epsilon_{\text{Nd}i}$ of ~ -1 and $\epsilon_{\text{Hf}i}$ of $\sim +3$). This endmember has He isotope characteristics consistent with continental lithospheric materials with long-term time-integrated high $(\text{U} + \text{Th})/^3\text{He}$ (Day et al. 2005; 2015), and Sr–Nd–Os isotope characteristics akin to lithospheric metasomes proposed for continental intraplate alkaline volcanic rocks elsewhere (e.g., Janney et al. 2002; Janney and Roex 2003; Rosenthal et al. 2009; Pfänder et al. 2018). Endmember (B) is consistent with metasomatized carbonate + phlogopite + amphibole-bearing peridotite, possibly existing as veins or heterogeneous pockets within peridotite with compositions like (A).

Regardless of the exact juxtaposition of the mantle sources of the FCC, the magmatic province extends isotopic variability in global continental intraplate alkaline volcanic rocks. In particular, FCC volcanic rocks originated from source compositions with higher time-integrated Lu/Hf for a given Sm/Nd ratio such that the compositions lie above the well-defined mantle array and is due to contributions from a high Lu/Hf carbonate source. The mantle-like $\delta^{18}\text{O}$ of most of the FCC volcanic rocks implies melts were in equilibrium with mantle peridotite and, as such, both the enriched and depleted mantle components are likely to exist in the lithosphere and/or asthenosphere. They do not require exotic recycled crustal origins, although metasomatic components that have evolved with high time-integrated Re/Os are required to explain the radiogenic Os isotope compositions (Day 2013). Furthermore, the radiogenic isotope compositions of FCC volcanic rocks support the idea that, rather than forming from similar mantle sources, continental intraplate alkaline volcanic rocks globally derive their distinct isotopic characteristics from the incorporation of variably aged and compositionally distinct lithospheric mantle sources.

An outcome of these comparisons is that continental intraplate alkaline volcanic rocks come from metasomatized sources that generally occur at the thermal boundary layer at the base of the lithosphere, where extent of partial melting plays an important role in controlling the extent to which enriched mantle sources are diluted by volumetrically more dominant lithospheric and/or asthenospheric peridotite mantle sourced melts. In the case of the FCC, there is no role for a deep mantle origin for the magmatism; other global

locations should be assessed for such contributions (e.g., Wilson et al. 1995; Rogers et al. 2000; Buikin et al. 2005; Zeng et al. 2021), specifically targeting He isotopes. The FCC offers some useful comparisons for global continental intraplate alkaline volcanic rocks as the trace-element evidence for hydrous phases (phlogopite and amphibole) and Hf isotope evidence for carbonate can also be associated with prior kimberlite magmatism in the region and, as such, metasomatic sources can be clearly defined (e.g., Fig. S10).

Implications for Arctic tectonics and magmatism

The Eurekan orogeny represents a period of deformation in the eastern portion of the Canadian Arctic and northern Greenland (e.g., Piepjohn et al. 2016). The orogeny coincides with spreading in the Labrador Sea at ~ 63 Ma and later in Baffin Bay, as well as in the Norwegian–Greenland Sea and Atlantic Ocean (see Gion et al. 2017 for summary). In this regard, a notable aspect of Bathurst Island is that it lies above a region of lithospheric mantle that is thin (< 100 km) based on surface and S wave forms, extending southeast towards the Labrador Sea (Schaeffer and Lebedev 2014; Lebedev et al., 2018). This contrasts with thicker lithosphere inferred for Ellesmere Island and N. Greenland or N. Baffin Island and Victoria Island. The absence of ancient lithospheric signatures in FCC volcanic rocks would suggest that, during the Eurekan orogeny, extension and thinning of the lithosphere reached Bathurst Island, although the thinning episode in this region was temporally restricted until ~ 54 Ma. It is likely that the period of extension was terminated due to a change from extension to compression in response to far field forces, in particular extension and seafloor spreading in the Arctic Ocean basin as well as the Norwegian–Greenland Sea. This is consistent with models of extension (Phase 1, 63–55 Ma) and compression (Phase 2, 55–35 Ma) suggested based on plate tectonic reconstructions (Gion et al. 2017). It is also notable that the timing of extension inferred from the FCC is broadly coincident with the start of the 55–45 Ma pulse of Central Lac de Gras field kimberlite magmatism far to the south on the Slave craton (Sarkar et al. 2015). Further study is warranted to investigate this temporal coincidence and the relationship of lithospheric metasomatism in this region more generally.

The FCC not only provides a time constraint (54–56 Ma) and evidence for extension followed by compression in the Canadian Arctic, but it also illustrates that the influence of the mantle flow associated with the Iceland mantle plume did not reach to Bathurst Island, providing a westerly limit to its influence. High- $^3\text{He}/^4\text{He}$ ratios have been measured in Eocene volcanic rocks from Baffin Island and west Greenland (Graham et al. 1998; Stuart et al. 2003)

surrounding the Labrador Sea, providing evidence for an Icelandic plume component to these rocks. The absence of similar signatures at the FCC illustrates that melting was likely to be the consequence of extension and that any inflowing mantle was local. Likewise, FCC volcanic rocks provide no compelling evidence for the extension of HALIP magmatism into the region into the Eocene. Previously, Tegner et al. (2011) argued that alkaline magmatism in the Arctic region from 85–60 Ma may be unrelated to the main tholeiitic stage of HALIP and was otherwise controlled by changes from extensional to compressional tectonics during the Late Cretaceous. The emplacement of the FCC further indicates that the change from extension to compression in the region surrounding Bathurst Island was likely to be ~54 Ma.

Conclusions

Partial melts spanning from melilitite to alkali basalt, along with phonolite differentiates, were erupted in the region of Bathurst Island (Nunavut, Canada) to form the Freemans Cove Complex (FCC) between ~56 and ~54 million years ago. The volcanic rocks comprising the FCC were erupted within a relatively small, localized extensional basin where low-degree partial melts appear to relate to the waxing (~56 Ma) and waning stages (~54 Ma) of incipient rifting, whereas higher degree partial melts are likely to have been emplaced during the main phase of rifting at ~55 Ma. Aside from some hydrothermally altered phonolites, most of the parental melts had $\delta^{18}\text{O}$ consistent with deriving from mantle peridotite sources. Two predominant mantle source components are evident beneath the FCC, a relatively depleted component (A; $^3\text{He}/^4\text{He} \sim 8 R_A$, $\epsilon_{\text{Nd}}^i \sim +3$, $\epsilon_{\text{Hf}}^i \sim +7$, $\gamma_{\text{Os}}^i \sim 0$) and an enriched component (B; $^3\text{He}/^4\text{He} < 3 R_A$, $\epsilon_{\text{Nd}}^i < -1$, $\epsilon_{\text{Hf}}^i < +3$, $\gamma_{\text{Os}}^i > +70$) that is sampled by low-degree partial melts and that represents metasomatized carbonate + phlogopite \pm amphibole-bearing peridotite. In detail, the depleted source was not like the depleted MORB mantle and may have also resided in the thermal boundary layer at the base of the lithosphere. Both sources may have formed a metasomatized vein-like mantle. Evolution of the mantle source, initially with Hf–Nd isotope compositions similar to Cretaceous Somerset Island kimberlites, could generate the distinctive isotopic signature in the ~40 Myr that elapsed between metasomatism of the source and magmatism, providing a link between kimberlite activity and later continental intraplate alkaline volcanic rocks formed in thinner lithosphere.

The FCC demonstrates that maximum extension from the Labrador Sea to Bathurst Island reached a zenith at ~55 Ma during the Eurekan orogeny, subsequently followed by cessation of rifting and termination of volcanism due to

Arctic plate tectonic reconfiguration. Isotopic signatures preserved in FCC volcanic rocks show that most of the melt generation occurred in relatively thinned (<100 km) lithosphere, at the lithosphere–asthenosphere boundary, with no mantle plume influence. In general, the melilitite to alkali basalt compositions of the FCC are like other continental intraplate alkaline volcanic rocks, such as products of the East African Rift or the Rhine Graben. In detail, however, the range of isotopic compositions preserved in low-degree partial melts associated with extension globally is likely to be dominated by temporal changes in extent of partial melting, as well as by the timing and degree of metasomatism recorded in the underlying continental lithosphere.

Supplementary Information The online version contains supplementary material available at <https://doi.org/10.1007/s00410-023-02068-y>.

Acknowledgements This work was partly done while JD, DGP, and AKB were at Durham University, and we are grateful for the opportunities offered there. Partial support also came from the Scripps Institution of Oceanography (JD) and a Canada Excellence Chair (DGP). Helicopter support for fieldwork was provided by the Polar Continental Shelf Project. BAK, NJ, and CJH acknowledge funding support from the Geological Survey of Canada. The reviews of J. Blusztajn and H. Sandeman and editorial comments of D. Canil were very helpful and are gratefully acknowledged.

Data availability All newly presented data are available in the supplementary tables associated with this article.

Open Access This article is licensed under a Creative Commons Attribution 4.0 International License, which permits use, sharing, adaptation, distribution and reproduction in any medium or format, as long as you give appropriate credit to the original author(s) and the source, provide a link to the Creative Commons licence, and indicate if changes were made. The images or other third party material in this article are included in the article's Creative Commons licence, unless indicated otherwise in a credit line to the material. If material is not included in the article's Creative Commons licence and your intended use is not permitted by statutory regulation or exceeds the permitted use, you will need to obtain permission directly from the copyright holder. To view a copy of this licence, visit <http://creativecommons.org/licenses/by/4.0/>.

References

- Ball PW, White NJ, Masoud A, Nixon S, Hoggard MJ, MacLennan J, Stuart FM, Oppenheimer C, Kröpelin S (2019) Quantifying asthenospheric and lithospheric controls on mafic magmatism across North Africa. *Geochem Geophys Geosyst* 20:3520–3555
- Bouvier A, Vervoort JD, Patchett PJ (2008) The Lu–Hf and Sm–Nd isotopic composition of CHUR: Constraints from unequilibrated chondrites and implications for the bulk composition of terrestrial planets. *Earth Planet Sci Lett* 273:48–57
- Bizimis M, Salters VJ, Dawson JB (2003) The brevity of carbonatite sources in the mantle: evidence from Hf isotopes. *Contrib Miner Petrol* 145:281–300

- Blusztajn J, Hegner E (2002) Osmium isotope systematics of melilitites from the Tertiary Central European Volcanic Province of SW Germany. *Chem Geol* 189:91–103
- Brey G (1978) Origin of olivine melilitites—chemical and experimental constraints. *J Volcanol Geoth Res* 3:61–88
- Buikink A, Trieloff M, Hopp J, Althaus T, Korochantseva E, Schwarz WH, Altherr R (2005) Noble gas isotopes suggest deep mantle plume source of late Cenozoic mafic alkaline volcanism in Europe. *Earth Planet Sci Lett* 230:143–162
- Canil D, Hyndman RD, Fode D (2021) Hygrometric control on the lithosphere–asthenosphere boundary: a 28 million year record from the Canadian Cordillera. *Geophys Res Lett* 48:e2020GL091957
- Carlson RW, Araujo ALN, Junqueira-Brod TC, Gaspar JC, Brod JA, Petrinovic IA, Hollanda MHB, Pimentel MM, Sichel S (2007) Chemical and isotopic relationships between peridotite xenoliths and mafic–ultrapotassic rocks from Southern Brazil. *Chem Geol* 242:415–434
- Carlson RW, Nowell GM (2001) Olivine-poor sources for mantle-derived magmas: Os and Hf isotopic evidence from potassic magmas of the Colorado Plateau. *Geochem Geophys Geosyst*. <https://doi.org/10.1029/2000GC000128>
- Day JMD (2013) Hotspot volcanism and highly siderophile elements. *Chem Geol* 341:50–74
- Day JMD, Hilton DR, Pearson DG, Macpherson CG, Kjarvsgaard BA, Janney PE (2005) Absence of a high time-integrated $^3\text{He}/(\text{U}+\text{Th})$ source in the mantle beneath continents. *Geology* 33:733–736
- Day JMD, Pearson DG, Macpherson CG, Lowry D, Carracedo J-C (2010) Evidence for distinct proportions of subducted oceanic crust and lithosphere in HIMU-type mantle beneath El Hierro and La Palma, Canary Islands. *Geochim Cosmochim Acta* 74:6565–6589
- Day JMD, Macpherson CG, Lowry D, Pearson DG et al (2012) Oxygen isotope heterogeneity of the mantle beneath Canary Islands: a discussion of the paper of Gurenko et al. *Contrib Miner Petrol* 164:177–183
- Day JMD, Peters BJ, Janney PE (2014) Oxygen isotope systematics of South African olivine melilitites and implications for HIMU mantle reservoirs. *Lithos* 202–203:76–84
- Dockman DM, Pearson DG, Heaman LM, Gibson SA, Sarkar C (2018) Timing and origin of magmatism in the Sverdrup Basin, Northern Canada—implications for lithospheric evolution in the High Arctic Large Igneous Province (HALIP). *Tectonophysics* 742:50–65
- Dowall DP (2004) Elemental and isotopic geochemistry of kimberlites from the Lac de Gras field, Northwest Territories, Canada. Ph.D. thesis, Durham University, p. 413
- Foley S (1992) Petrological characterization of the source components of potassic magmas: Geochemical and experimental constraints. *Lithos* 28:187–204
- Foley SF, Yaxley GM, Kjarvsgaard BA (2019) Kimberlites from source to surface: insights from experiments. *Elements* 15:393–398
- Frey FA, Green DH, Roy SD (1978) Integrated models of basalt petrogenesis: a study of quartz tholeiites to olivine melilitites from south eastern Australia utilizing geochemical and experimental petrological data. *J Petrol* 19:463–513
- Genske FS, Beier C, Haase KM, Turner SP, Krumm S, Brandl PA (2013) Oxygen isotopes in the Azores islands: Crustal assimilation recorded in olivine. *Geology* 41:491–494
- Gion AM, Williams SE, Muller RD (2017) A reconstruction of the Eureka orogeny incorporating deformation constraints. *Tectonics* 36:304–320
- Gräf C, Woodland A, Höfer H, Seitz HM, Pearson G, Kjarvsgaard B (2019) Metasomatism and oxidation state of the lithospheric mantle beneath the Rae craton, Canada as revealed by xenoliths from Somerset Island and Pelly Bay. In: *Geophysical Research Abstracts* (Vol. 21)
- Graham DW, Larsen LM, Hanan BB, Storey M, Pedersen AK, Lupton JE (1998) Helium isotope composition of the early Iceland mantle plume inferred from the Tertiary picrites of West Greenland. *Earth Planet Sci Lett* 160:241–255
- Harrison JC (2018) Intersecting fold belts in the Bathurst Island region, Nunavut. *J Geodyn* 118:82–105
- Harrison JC, Mayr U, McNeil DH, Sweet AR, Eberle JJ, McIntyre DJ, Harington CR, Chalmers JA, Dam G, Nøhr-Hansen H (1998) Correlation of Cenozoic sequences of the Canadian Arctic region and Greenland; implications for the tectonic history of northern North America. *Bull Can Pet Geol* 47(3):223–254
- Hirschmann MM, Renne PR, McBirney AR (1997) ^{40}Ar – ^{39}Ar dating of the Skaergaard intrusion. *Earth Planet Sci Lett* 146(3–4):645–658
- Irvine GJ, Pearson DG, Kjarvsgaard BA, Carlson RW, Kopylova MG, Dreibus G (2003) A Re–Os and PGE study of kimberlite-derived peridotite xenoliths from Somerset Island and a comparison to the Slave and Kaapvaal cratons. *Lithos* 71:461–488
- Janney PE, le Roex AP, Carlson RW, Viljoen KS (2002) A chemical and multi-isotope study of the Western Cape olivine melilitite province, South Africa: Implications for the sources of kimberlites and the origin of the HIMU signature in Africa. *J Petrol* 43:2339–2370
- Janney PE, le Roex AP, Carlson RW, Bell DR (2003) Os and Hf isotopic constraints on the sources of olivine melilitites from western South Africa. In: *8th International Kimberlite Conference Extended Abstracts*, Victoria, British Columbia, Canada, p 127 (CD-ROM)
- Jung S, Pfänder JA, Brauns M, Maas R (2011) Crustal contamination and mantle source characteristics in continental intraplate volcanic rocks: Pb, Hf and Os isotopes from Central European Volcanic Province basalts. *Geochim Cosmochim Acta* 75:2664–2683
- Kerr JW (1974) Geology of Bathurst Island Group and Byam Martin Island, Arctic Canada (**Operation Bathurst Island**)
- Kjarvsgaard BA, Heaman LM, Sarkar C, Pearson DG (2017) The North America mid-Cretaceous kimberlite corridor: Wet, edge-driven decompression melting of an OIB-type deep mantle source. *Geochem Geophys Geosyst* 18:2727–2747
- Le Bas MJ (1987) Nephelinites and carbonatites. *Geol Soc Lond Spec Publ* 30:53–83
- Lebedev S, Schaeffer AJ, Fullea J, Pease V (2018) Seismic tomography of the Arctic region: inferences for the thermal structure and evolution of the lithosphere. *Geol Soc Lond Spec Publ* 460:419–440
- Liu J, Brin L, Pearson DG, Bretschneider L, Luguet A, van Acken D, Kjarvsgaard BA, Riches A, Miskovic A (2018) Diamondiferous Paleoproterozoic mantle roots beneath Arctic Canada: A study of mantle xenoliths from Parry Peninsula and Central Victoria Island. *Geochimica et Cosmochimica Acta* 239:284–311
- Macpherson CG, Hilton DR, Day JMD, Lowry D, Grönvold K (2005) High- $^3\text{He}/^4\text{He}$, depleted mantle and low- $\delta^{18}\text{O}$, recycled oceanic lithosphere in the source of central Iceland magmatism. *Earth Planet Sci Lett* 233:411–427
- Marty B, Upton B, Ellam R (1998) Helium isotopes in early Tertiary basalts, northeast Greenland: evidence for 58 Ma plume activity on the North Atlantic–Iceland volcanic province. *Geology* 26:407–410
- Mattey DP, Lowry D, Macpherson C (1994) Oxygen isotope composition of mantle peridotite. *Earth Planet Sci Lett* 128:231–241
- McDonough WF, Sun S-S (1995) The composition of the Earth. *Chem Geol* 120:223–253
- Mckenzie D, Bickle MJ (1988) The volume and composition of melt generated by extension of the lithosphere. *J Petrol* 29:625–679
- Mitchell RH, Platt RG (1983) Primitive nephelinitic volcanism associated with rifting and uplift in the Canadian Arctic. *Nature* 303:600–612

- Mitchell RH, Platt RG (1984) The Freemans Cove volcanic suite: field relations, petrochemistry, and tectonic setting of nephelinite-basanite volcanism associated with rifting in the Canadian Arctic archipelago. *Can J Earth Sci* 21:428–436
- Nisbet EG, Cheadle MJ, Arndt NT, Bickle MJ (1993) Constraining the potential temperature of the Archaean mantle: a review of the evidence from komatiites. *Lithos* 30:291–307
- Pfänder JA, Jung S, Klügel A, Müunker C, Romer RL, Sperner B, Rohrmüller J (2018) Recurrent local melting of metasomatized lithospheric mantle in response to continental rifting: constraints from basanites and nephelinites/melilitites from SW Germany. *J Petrol* 59:667–694
- Piejohn K, Von Gosen W, Tessensohn F (2016) The Eurekan deformation in the Arctic: an outline. *J Geol Soc* 173:1007–1024
- Pilet S, Baker MB, Stolper EM (2008) Metasomatized lithosphere and the origin of alkaline lavas. *Science* 320:916–919
- Rogers N, Macdonald R, Fitton JG, George R, Smith M, Barreiro B (2000) Two mantle plumes beneath the East African rift system: Sr, Nd and Pb isotope evidence from Kenya Rift basalts. *Earth Planet Sci Lett* 176:387–400
- Rosenthal A, Foley SF, Pearson DG, Nowell GM, Tappe S (2009) Petrogenesis of strongly alkaline primitive volcanic rocks at the propagating tip of the western branch of the East African Rift. *Earth Planet Sci Lett* 284:236–248
- Sarkar C, Heaman LM, Pearson DG (2015) Duration and periodicity of kimberlite volcanic activity in the Lac de Gras kimberlite field, Canada and some recommendations for kimberlite geochronology. *Lithos* 218:155–166
- Schaeffer AJ, Lebedev S (2014) Imaging the North American continent using waveform inversion of global and USArray data. *Earth Planet Sci Lett* 402:26–41
- Spencer AB (1969) Alkaline igneous rocks of the Balcones province, Texas. *J Petrol* 10:272–306
- Stuart FM, Lass-Evans S, Fitton JG, Ellam RM (2003) High $3\text{He}/4\text{He}$ ratios in picritic basalts from Baffin Island and the role of a mixed reservoir in mantle plumes. *Nature* 424:57–59
- Tappe S, Pearson DG, Kjarsgaard BA, Nowell G, Dowall D (2013) Mantle transition zone input to kimberlite magmatism near a subduction zone: origin of anomalous Nd–Hf isotope systematics at Lac de Gras, Canada. *Earth Planet Sci Lett* 371:235–251
- Taylor HP, Forester RW (1971) Low- O^{18} igneous rocks from the intrusive complexes of Skye, Mull, and Ardnamurchan, Western Scotland. *J Petrol* 12:465–497
- Tegner C, Duncan RA, Bernstein S, Brooks CK, Bird DK, Storey M (1998) ^{40}Ar – ^{39}Ar geochronology of Tertiary mafic intrusions along the East Greenland rifted margin: Relation to flood basalts and the Iceland hotspot track. *Earth Planet Sci Lett* 156:75–88
- Tegner C, Storey M, Holm PM, Thorarinsson SB, Zhao X, Lo CH, Knudsen MF (2011) Magmatism and Eurekan deformation in the High Arctic large igneous province: ^{40}Ar – ^{39}Ar age of Kap Washington Group volcanics, North Greenland. *Earth Planet Sci Lett* 303:203–214
- Thompson RN, Ottley CJ, Smith PM, Pearson DG, Dickin AP, Morrison MA, Leat PT, Gibson SA (2005) Source of the quaternary alkalic basalts, picrites and basanites of the Potrillo Volcanic Field, New Mexico, USA: lithosphere or convecting mantle? *J Petrol* 46:1603–1643
- Veizer J (1989) Strontium isotopes in seawater through time. *Annu Rev Earth Planet Sci* 17:141
- Vervoort JD, Patchett PJ, Blichert-Toft J, Albarède F (1999) Relationships between Lu–Hf and Sm–Nd isotopic systems in the global sedimentary system. *Earth Planet Sci Lett* 168:79–99
- Vollmer R, Norry MJ (1983) Unusual isotopic variations in Nyiragongo nephelinites. *Nature* 301:141–143
- Weisenberger TB, Spürigin S, Lahaye Y (2014) Hydrothermal alteration and zeolitization of the Föhberg phonolite, Kaiserstuhl Volcanic Complex, Germany. *Int J Earth Sci* 103:2273–2300
- Wilson M, Rosenbaum JM, Dunworth EA (1995) Melilitites: partial melts of the thermal boundary layer? *Contrib Miner Petrol* 119:181–196
- Zeng G, Chen L-H, Hofmann AW, Wang X-J, Liu J-Q, Yu X, Xie L-W (2021) Nephelinites in eastern China originating from the mantle transition zone. *Chem Geol* 576:120276
- Zheng Y-F (1993) Calculation of oxygen isotope fractionation in anhydrous silicate minerals. *Geochim Cosmochim Acta* 57:1079–1091

Publisher's Note Springer Nature remains neutral with regard to jurisdictional claims in published maps and institutional affiliations.